Bull. Mater. Sci., Vol. 38, No. 4, August 2015, pp. 945–950. © Indian Academy of Sciences.

Biosynthesis of Yttrium oxide nanoparticles using *Acalypha indica* leaf extract

S K KANNAN and M SUNDRARAJAN*

Advanced Green Chemistry Lab, Department of Industrial Chemistry, School of Chemical Sciences, Alagappa University, Karaikudi 630 003, Tamil Nadu, India

MS received 7 July 2014; accepted 3 February 2015

Abstract. **In this study, the synthesis of Yttrium oxide (Y_2O_3) nanoparticles was carried out from *Acalypha indica* leaf extract. The synthesized nanoparticles were characterized by using X-ray diffraction, scanning electron microscope, energy-dispersive X-ray spectrometer and transmission electron microscope for structural confirmation. The studies clearly indicate that the synthesized Y_2O_3 nanoparticle is a crystalline material with a particle size from 23 to 66 nm. Further analysis was carried out by Fourier transform infrared spectroscopy, to provide the evidence for the presence of Y–O–Y and O–Y–O stretchings in the synthesized Y_2O_3 nanoparticles. Thermogravimetric and differential scanning calorimetry analyses gave the thermal stability of Y_2O_3 nanoparticles. The results of the antibacterial studies conducted by using the synthesized Y_2O_3 revealed an increasing rate of antibacterial behaviour with pathogens.**

Keywords. **Yttrium oxide; biosynthesis; nanostructure; *Acalypha indica*; antibacterial activity.**

1. Introduction

Nanosized metal oxides, in a variety of morphologies (such as particles, spheres, rods and sheets) have attracted a great deal of attention. This is owing mainly to their physico-chemical properties associated with their technological application. Synthesis of nanosized material is one of the major challenges in the development of advanced functional materials because they exhibit unique properties conferred by particles of very small dimension in contrast to the corresponding bulk material.[1–3] Interest in nanoparticles for biological and medical applications continues to grow. Nanoparticles find use as delivery vehicles for drugs,[4,5] genes[6,7] and growth factor[8] as well as cellular labels for imaging both *in vitro* and *in vivo*.[9–11] Nanoparticles are also being studied for the use in photodynamic therapy[12] and hyperthermia therapy for tumour,[13] with the goal of clinical application.

Nowadays biosynthesis plays a vital role in the synthesis of metal and metal oxide nanoparticles. It eliminates toxic chemicals which are formed as by-products in certain chemical reactions and removes the organic solvent in the synthetic protocol. Green synthesis offers improvement over synthetic, chemical or microbiological methods as it is cost effective, environmental friendly and can easily be scaled up for large-scale synthesis. Although biosynthesis of metal and metal oxide nanoparticles by plants such as *Alfalfa*,[14,15] *Aloe vera*,[16] *Cinnamomum camphora*,[17] *Emblica officianalis*,[18] have been reported, the potential plants as biological materials for the synthesis of nanoparticles is yet to be fully explored.

Yttrium oxide (Y_2O_3), as an important member among rare earth compounds, has been actively studied in the recent years. It is one of the most promising elements for the fabrication of optoelectronic devices and chemical catalysis. Y_2O_3 is a well-known material for its characteristics of high dielectric constant and good thermal stability in a powder state.[19] Y_2O_3 can be used as high efficient additives and functional composite materials like yttria-stabilized zirconia films.[20,21] In addition to that, it is widely used as a host material for various rare earth dopants and is of interest for potential applications in biological imaging as well as photodynamic therapy.[22,23]

The aim of this work is to study the processes taking place in the precipitation of yttrium hydroxides from nitrate solutions by using *Acalypha indica* leaf extracts as a precipitant, the thermal decomposition of precipitates with the production of Y_2O_3 and the evolution of particle ensembles in the processes of thermal processing. The synthesized pure Y_2O_3 nanoparticles were characterized by X-ray diffraction (XRD), scanning electron microscope (SEM), transmission electron microscope (TEM), enery-dispersive X-ray (EDX) spectrometer, Fourier transform infrared (FT-IR) spectroscopy and thermogravimetric analysis (TGA)–differential scanning calorimetry (DSC) analyses. Further the Y_2O_3 nanoparticle was tested for its antibacterial activity with human pathogens.

*Author for correspondence (sundrarajan@yahoo.com)

2. Experiment

2.1 *Material*

Yttrium nitrate hexahydrate [$Y(NO_3)_3{\cdot}6H_2O$] purchased from Alfa Aesar was directly used without further purification. The leaves of *A. indica* were collected in the Alagappa University Campus, India, washed thoroughly with double distilled water and dried for a week at room temperature.

2.2 *Preparation of plant extract*

The dried and finely cut leaves (20 g) were boiled in a 250 ml Erlenmeyer flask with 100 ml of double distilled water for 30 min. Then the extract was filtered through ordinary filter paper and through Whatman No. 1 filter paper. The filtrate was collected and it was kept in a refrigerator at 4°C for further experiments.

2.3 *Synthesis of Y_2O_3 nanoparticle*

Aqueous solution of 0.1 M yttrium nitrate hexahydrate [$Y(NO_3)_3{\cdot}6H_2O$] was used for the synthesis of Y_2O_3 nanoparticles. Briefly, 10 ml of *A. indica* leaf extract was added to 50 ml of 0.1 M $Y(NO_3)_3{\cdot}6H_2O$ in a 250 ml Erlenmeyer flask and stirred at 80°C for 2 h. The particle formed after adequate time of stirring was collected by centrifugation at 10,000 rpm for 10 min. The centrifuged particles were washed with deionized water and again subjected to centrifugation at 1500 rpm for 30 min. The centrifuged sample, dried in an air oven, was powdered using mortar and pestle. This powdered sample was calcined in a muffle furnace at 500°C to obtain Y_2O_3 nanoparticles.[24]

2.4 *Characterization*

SEM images were obtained using HITACHI Model S-3000H at various magnifications to study the surface morphology of Y_2O_3 nanoparticles. XRD data sets were recorded at room temperature on a PANalytical X'PERT PRO system in Bragg–Brentano geometry using CuKα1 (1.540 Å) radiation. The powder diffraction covered the $10° < 2\theta > 40°$ range with 0.0170° steps. FT-IR spectra were obtained using BRUKER Optik GmbH FTIR spectrometer model TENSOR 27 in the diffuse reflection mode. The TEM images were recorded by using PHILIPS CM 200, operating voltage 20–200 kV with resolution range at 2.4 Å. TGA–DSC reports were collected by using TGA–DSC Perkin Elmer Instruments under nitrogen flow condition.

2.5 *Antibacterial activity study*

2.5a *Disc diffusion method*: *Escherichia coli* (*E. coli*), *Pseudomonas aeruginosa* (*P. aeruginosa*), *Serratia marcescens* (*S. marcescens*) and *Staphylococcus aureus* (*S. aureus*) cultures were used for this study as reference strains used for antimicrobial susceptibility testing by the Kirby–Bauer diffusion method. The bacterial suspension was applied uniformly on the surface of a Muller Hinton agar (MHA) plate in the concentration range of 10^5–10^6 CFU ml^{-1} before placing Y_2O_3 nanoparticle laden disk. The strains were cultured on nutrient agar (Himedia, India) and incubated aerobically at 35°C overnight.

2.5b *Turbidimetric method*: The antibacterial activity of the Y_2O_3 nanoparticles was justified by an alternative route like the turbidimetric method. In this method, the antibacterial behaviour of Y_2O_3 against *E. coli, P. aeruginosa, S. marcescens* and *S. aureus* in Luria Bertani broth (LB). The 24-h-old bacterial cultures were inoculated into LB broth supplemented with various concentrations (10, 15, 25, 50, 75 and 100 µl) of Y_2O_3 nanoparticles. Y_2O_3-free LB broth was used as a control. The broth containing conical flasks was incubated at room temperature under stirring for 24 h and the vulnerability of the tested organisms was observed by taking optical density at 600 nm for various time intervals.

3. Results and discussion

XRD has been used to characterize the structure of Y_2O_3 nanoparticle. Figure 1 shows a typical diffraction pattern of this material. This could clearly demonstrate that, the synthesized Y_2O_3 nanoparticle is identical and could be indexed to the standard Y_2O_3 with body centered cubic structure (JCPDS no: 89-5591). The lattice parameter calculated from (222) Bragg's reflection of the pure Y_2O_3 nanoparticle sample is 10.62 Å which matches well with the lattice parameter of bulk Y_2O_3 ($a = 10.60$). Some minor peaks appeared in an XRD data due to traces of other impurities were observed in the XRD pattern after calcined at 500°C in the air.

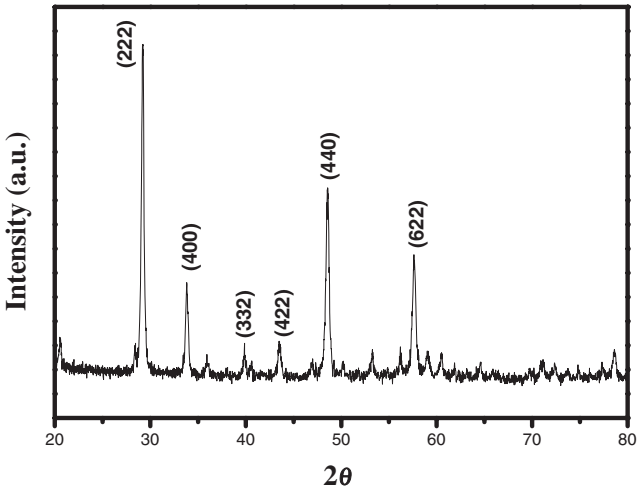

Figure 1. XRD pattern of the synthesized Y_2O_3 nanoparticles using *Acalypha indica* leaf extract.

The crystallite size of Y_2O_3 nanoparticle was estimated from Scherrer's equation as 33.5 nm.

The FT-IR spectrum of Y_2O_3 made from KBr pellet is shown in figure 2. There is an absorption peak at 3393, 1607, 1384, 1175, 1072, 1010, 881, 578 and 459 cm^{-1}. The peak at 3393 cm^{-1} corresponds to stretching vibration of O–H bonds in H_2O molecules and the band at 1607 cm^{-1} could be attributed to in-plane and out-of-plane bending of O–H bonds present in the adsorbed water molecule. The peaks at 1175, 1072 and 1010 cm^{-1} are the characteristic asymmetric stretching of Y–O–Y present in the nanostructure. The peak at 881 cm^{-1} is responsible for the presence of trace of Y–OH. The intense peak at 578 cm^{-1} corresponds to the anti-symmetric Y–O–Y stretching mode of the surface–bridging oxide. The peak at 459 cm^{-1} corresponds to symmetric stretching O–Y–O linkage present in Y_2O_3 nanoparticles.

The morphology of the synthesized Y_2O_3 was examined by SEM and the images are presented in figure 3. It is clear from the figures that a non-defined morphology of the agglomerated particles is seen and the particles could not be resolved even at high magnification. This is due to the high surface energy of nanoparticles there tendency to form agglomerates are quite strong. Upon contact the primary particles of agglomerate form bonds, which can be of different nature. Sintering and individual particle adsorption from the surrounding atmosphere can lead to solid state necks.

Analysis through EDX spectrometer has confirmed the presence of elemental yttrium and the oxygen signal of the Y_2O_3 nanoparticles figure 4. The vertical axis displays the number of X-ray counts while the horizontal axis displays energy in keV. Identification lines for the major emission energies of yttrium and oxygen are displayed and these correspond to peaks in the spectrum, thus giving confidence that yttrium and oxygen has been correctly identified.

A more detailed structural analysis was performed by TEM analysis. A global view of the Y_2O_3 nanoparticle at lower magnification is depicted in figure 5. The morphology of the Y_2O_3 nanoparticles was ununiformed with distributed elliptically spherical particles with various sizes ranging from 23 to 64 nm. This is because the nanoparticles are agglomerated and the necking between particles examined to determine the particle are sintered together. If the particles are sintered, the diameter of the particle is measured at a fixed angle for all particles in the image. Most of the nanoparticles were well arranged although some of them are partially aggregated. However, TEM analysis illustrates sheet- and spherical-like particles of nearly uniform size. However, agglomeration of particles is also evident from the TEM pictures.

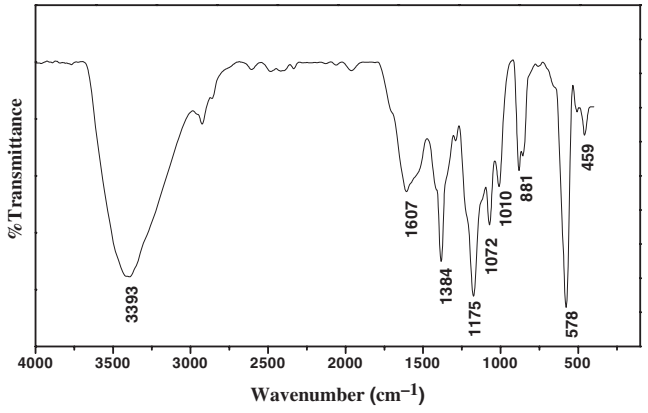

Figure 2. FT-IR spectra of the synthesized Y_2O_3 nanoparticles using *Acalypha indica* leaf extract.

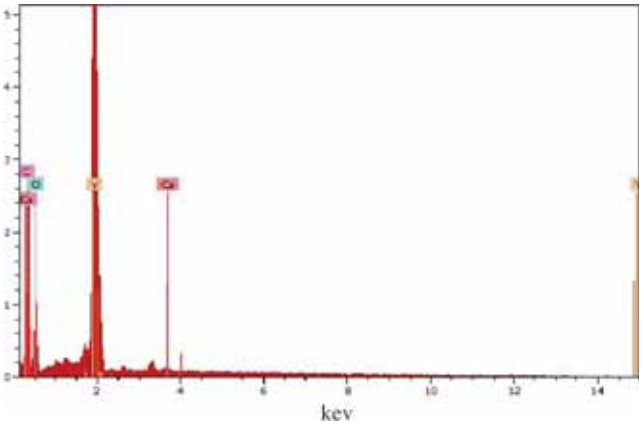

Figure 4. EDX spectrum of the synthesized Y_2O_3 nanoparticles using *Acalypha indica* leaf extract.

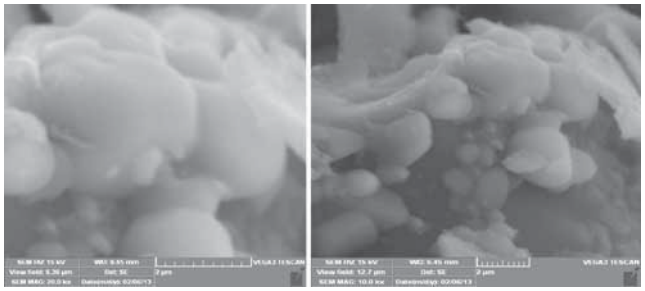

Figure 3. SEM micrograph of the synthesized Y_2O_3 nanoparticles using *Acalypha indica* leaf extract.

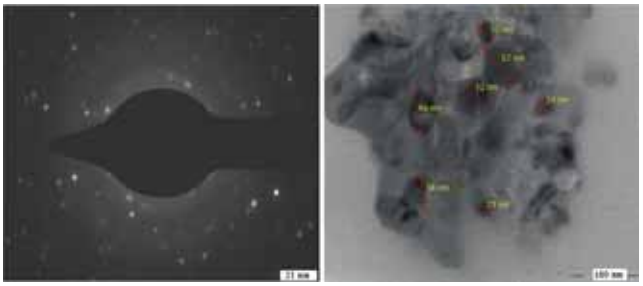

Figure 5. TEM images of the synthesized Y_2O_3 nanoparticles using *Acalypha indica* leaf extract.

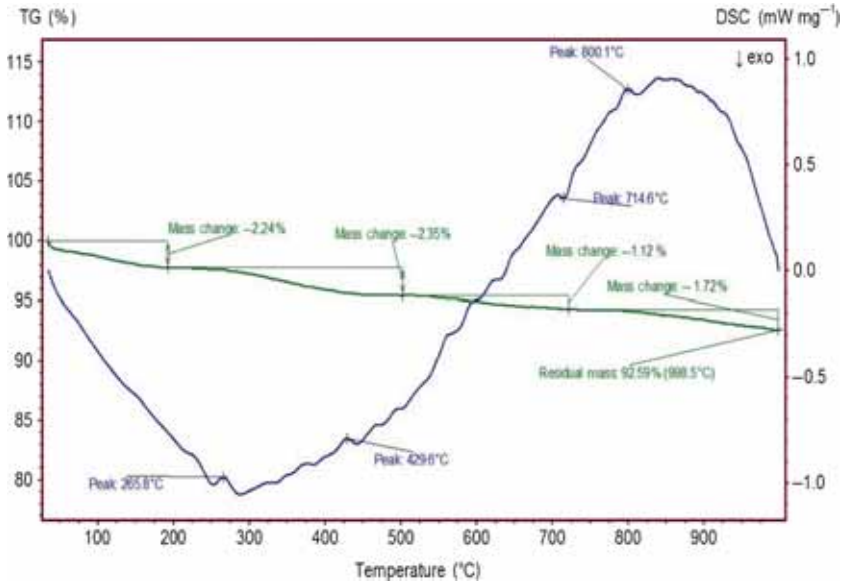

Figure 6. TG-DSC curves of the synthesized Y_2O_3 nanoparticles using *Acalypha indica* leaf extract.

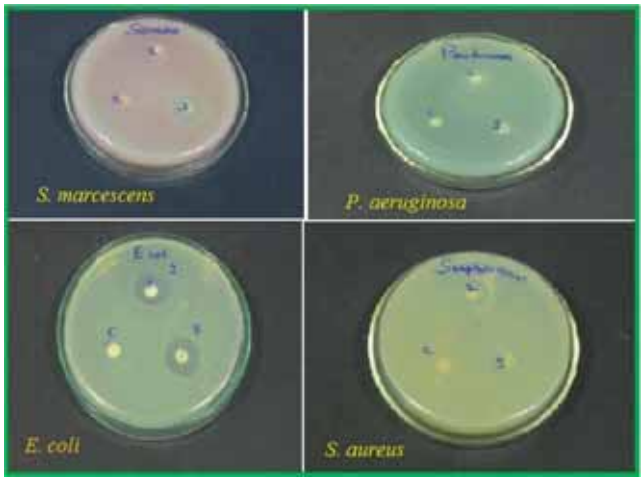

Figure 7. Antibacterial behaviour of the synthesized Y_2O_3 nanoparticles using *Acalypha indica* leaf extract.

In figure 6, the TGA/DSC plot acquired for the decomposition of the Y_2O_3 nanoparticle is presented. The sample was heated at a constant rate under N_2 atmosphere with range of 35°C/10.0 (k min^{-1})/1000°C. It is important to use an inert gas for performing such a study to avoid any premature oxidation and/or capping agent combustion. In TGA analysis, there is a gradual weight loss up to 200°C indicates that the removal of water molecules adsorbed on the nanoparticle and then slight increase of weight loss up to 700°C denotes the breakdown of the evaporation of physically and chemically adsorbed water and present in the nanoparticle. On further heating, no significant weight loss was observed supporting the crystallinity of particle takes place at 998°C. In DSC analysis, a broad endothermic peak at 265°C indicates the evolving of water molecules. The curing temperature range from 429 to 714°C indicates the gradual removal of adsorbed water molecule on the Y_2O_3 nanoparticle. An exothermic peak at 800°C, supports the formation of crystalline particles with phase-chemical purity. Based on these studies, the synthesized nanoparticles were thermally more stable. It was observed that the morphologies of nanoparticles can be controlled with the help of reaction methodology and type of solvents used.

3.1 *Antibacterial activity of Y_2O_3 nanoparticle*

The antibacterial activity of Y_2O_3 nanoparticle was examined against four representative microorganisms *S. marcescens, P. aeruginosa, E. coli* and *S. aureus*. *S. marcescens* is a common bacterium that can cause disease in humans and animals. It is found in soil, water, skin flora, and most man-made environments throughout the world. *P. aeruginosa* is involved in hospital acquired infections (HAIs), particularly catheter-associated bacteraemia, urinary tract infections and wound infection. *E. coli*, the most characterized bacterium, has been used as a model bacterial system for various antibacterial testing programs. *S. aureus* is responsible for the wide range of infectious diseases ranging from benign skin infections to life-threatening endocarditis and toxic shock syndrome. In a disc diffusion method, the Y_2O_3 nanoparticles laden disk has been prepared by keeping the disks in 5 ml colloidal solutions of Y_2O_3 nanoparticles for 2 days. These disks absorb the Y_2O_3 nanoparticles and become dry and hence there is no presence of chloroform. Hence there is no impact of solvent to the bacteria. The plates with the disk were incubated at 35°C for 24 h, after which the average diameter of the inhibition zone surrounding the disk was measured with a ruler. Figure 7 shows plates to which *E. coli, P. aeruginosa, S. marcescens* and *S.*

aureus bacterial suspension were applied with nanoparticles laden disk and antibiotic impregnated disks. The diameter of inhibition zones around the disk containing Y_2O_3 nanoparticles in *E. coli*, *P. aeruginosa*, *S. marcescens* and *S. aureus* bacterial suspension are 11, 10, 10 and 13 mm, respectively.

The antibacterial effects of Y_2O_3 nanoparticles solutions can also be measured by determining the minimum concentration needed to inhibit the growth of tested microorganisms. Minimum inhibitory concentration (MIC) values of Y_2O_3 nanoparticles solutions against test microorganisms are given in table 1. This shows that all tested microorganisms were completely inhibited at the concentration of 8–12 μg ml^{-1} of Y_2O_3 nanoparticles. Y_2O_3 nanoparticles solution at the concentration of 8 μg ml^{-1} showed inhibition kinetics against *E. coli* and *P. aeruginosa* while 9 μg ml^{-1} of nano-Y_2O_3 was found to be the most effective against *S. marcescens*. The MIC of nano-Y_2O_3 against *S. aureus* was also 14 μg ml^{-1}. Thus, we can conclude from the results of this study that Y_2O_3 nanoparticles inhibited the growth and multiplication of all the tested microorganisms effectively.

Table 1. MIC of yttrium oxide nanoparticle solution against tested pathogens (μg ml^{-1}).

	E. coli	*P. aeruginosa*	*S. marcescens*	*S. aureus*
MIC of nanosized yttrium oxide solution (μg ml^{-1})	8	8	9	14

Figure 8 shows the growth curves of *E. coli*, *P. aeruginosa*, *S. marcescens* and *S. aureus* in LB broth. The inhibitory effect of various concentrations of Y_2O_3 nanoparticles (10, 15, 25, 50, 75 and 100 μl) was examined through UV–visible spectrophotometer by taking optical density (OD) values. The growth rate of biomass was compared with the addition of Y_2O_3 nanoparticles with biomass. The growth rate of *E. coli, P. aeruginosa, S. marcescens* and *S. aureus* was decreased at the increased concentration of Y_2O_3 nanoparticles and the maximum inhibition of growth was obtained at 100 μl.

The mechanism of the bactericidal effect of Y_2O_3 nanoparticles is not very well-known. It is believed that cellular proteins become inactive after treatment with Y_2O_3 nanoparticles. It is also believed that Y_2O_3 nanoparticles after penetration into the bacteria have inactivated their enzymes, generating hydrogen peroxide and caused bacterial cell death. Heavy metals are toxic and react with proteins, therefore they bind protein molecules; as a result, cellular metabolism is inhibited causing death of the microorganism. Our experimental result shows that Y_2O_3 nanoparticles can be used as effective growth inhibitors in various microorganisms, making them applicable to diverse medical medicines and antimicrobial control systems.

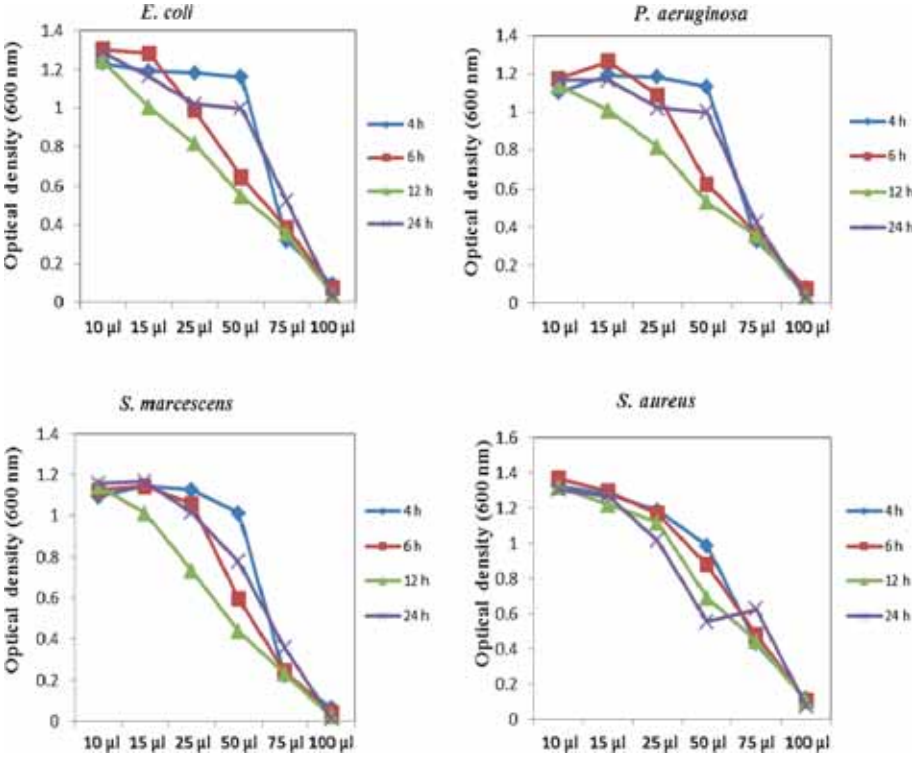

Figure 8. Growth curves of *E. coli*, *P. aeruginosa, S. marcescens* and *S. aureus*, LB broth containing various concentrations of the synthesized Y_2O_3 nanoparticles using *Acalypha indica* leaf extract.

4. Conclusion

The present paper describes that the extract of *A. indica* leaf is capable of producing yttrium oxide nanoparticles from precursor material which are quite stable in solution. The authors proudly say that this is a first paper to describe the biosynthesis of Y_2O_3 nanoparticles. Y_2O_3 nanoparticles are much more stable upon treatment of thermal analysis and also it gives good antibacterial activity against the microorganisms such as *S. marcescens, P. aeruginosa*, *E. coli* and *S. aureus*. The achievement of such green synthesis of Y_2O_3 nanoparticle, contributes the rise of synthetic procedures using environmentally benign natural resources.

Acknowledgement

I gratefully acknowledge Dr M Anbu Kulandainathan and Dr K Kulangiappar, Scientist, Central Electrochemical Research Institute, Karaikudi, India, for their valuable suggestions during this part of my research work.

References

1. Martin C R 1994 *Science* **266** 1961
2. Mathur S, Shen H, Lecerf N, Kjekshus A, Fjellvag H and Goya G F 2002 *Adv. Mater.* **14** 1405
3. Wu L, Yu L C, Zhang L, Wang X and Li S 2004 *J. Solid State Chem.* **177** 3666
4. Soppimath K S, Aminabhavi T M, Kulkarni A R and Rudzinski W E 2001 *J. Control. Release* **70** 1
5. Kreuter J 2001 *Adv. Drug Deliv. Rev.* **47** 65
6. Hood J D, Bednarski M, Frausto R, Guccione S, Reisfeld R A, Xiang R and Cheresh D A 2002 *Science* **296** 2404
7. Mao H Q, Roy K, Troung-Le V L, Janes K A, Lin K Y, Wang Y, August J T and Leong K W 2001 *J. Control. Release* **70** 399
8. Chung Y I, Tae G and Yuk S H 2006 *Biomaterials* **27** 2621
9. Gao X H, Cui Y Y, Levenson R M, Chung L W K and Nie S M 2004 *Nat. Biotechnol.* **22** 969
10. Akerman M E, Chan W C W, Laakkonen P, Bhatia S N and Ruoslahti E 2002 *Proc. Natl. Acad. Sci.* **99** 12617
11. Gao X H, Yang L L, Petros J A, Marshal F F, Simons J W and Nie S M 2005 *Curr. Opin. Biotechnol.* **16** 63
12. Roy I, Ohulchanskyy T Y, Pudavar H E, Bergey E J, Oseroff A R, Morgan J, Dougherty T J and Prasad P N 2003 *J. Am. Chem. Soc.* **125** 7860
13. Mornet S, Vasseur S, Grasset F and Duguet E 2004 *J. Mater. Chem.* **14** 2161
14. Gardea-Torresdey J L, Parsons J G, Gomez E, Peralta-Videa J, Troiani H E and Santiago P 2002 *Nano Lett.* **2** 397
15. Gardea-Torresdey J L, Parsons J G, Gomez E, Peralta-Videa J and Troiani H E 2003 *Langmuir* **13** 1357
16. Chandran S P, Chaudhary M, Pasricha R, Ahmad A and Sastry M 2006 *Biotechnol. Prog.* **22** 577
17. Huang J, Li Q, Sun D, Lu Y, Su Y and Yang X 2007 *Nanobiotechnology* **18** 105
18. Ankamwar B, Chinmay D, Absar A and Murali S 2005 *J. Nanosci. Nanotechnol.* **10** 1665
19. Hirai T, Kawamura Y and Komasawa I 2004 *J. Colloid Interface Sci.* **275** 508
20. Verhiest K, Almazouzi A, Wispelaere N, Petrov R and Claessens S 2009 *J. Nucl. Mater.* **385** 308
21. Wang Z C and Kim K B 2008 *Mater. Lett.* **62** 425
22. Chang M L and Tie S L 2008 *Nanotechnology* **19** 075711
23. Andelman T, Gordonov S, Busto G, Moghe P V and Riman R E 2010 *Nanoscale Res. Lett.* **5** 263
24. Sathishkumar M, Sneha K, Won S W, Cho C W, Kim S and Yun Y S 2009 *Colloids Surf. B* **73** 332